

Metallicity gradients with Galactic PNe using Gaia DR3

Beatrice Bucciarelli¹, Letizia Stanghellini²

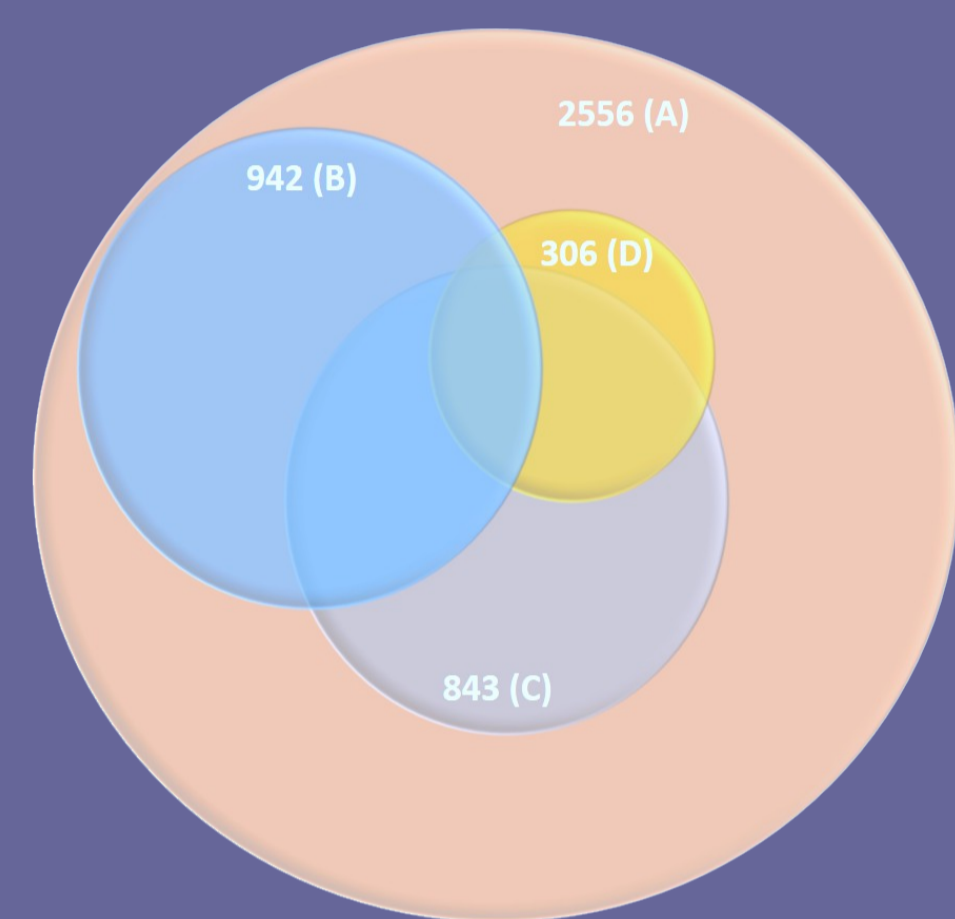
¹INAF-OATo: Istituto Nazionale di AstroFisica – Osservatorio Astrofisico di Torino, ²NFS's NOIRLab, Tucson AZ, USA

INAF
ISTITUTO NAZIONALE
DI ASTROFISICA
NATIONAL INSTITUTE
FOR ASTROPHYSICS

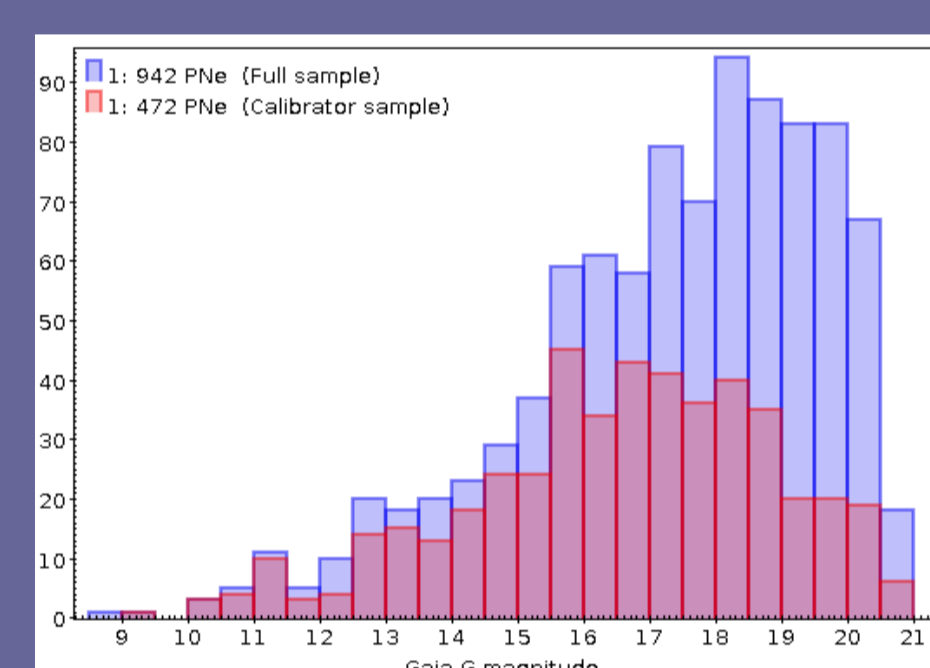
Gaia DR3 parallaxes of a well constrained sample of confirmed central stars (CSPNs) of Galactic planetary nebulae (PNe) with available angular radius and flux measurements are employed to recalibrate one of the classical PN statistical distance scales. Oxygen-to-hydrogen spectral abundance of ~250 Galactic PNe, having either young (< 1 Gyr) or old (> 7.5 Gyr) CSPN progenitors, whose distances are obtained with the new scale are then used as tracers of the radial metallicity profile of the Galactic disk. We confirm a negative slope of the complete PN sample, finding a mild steepening of the gradient since Galaxy formation.

CONTEXT Planetary Nebulae are asymptotic giant branch (AGB) stellar ejecta of low-to-intermediate-mass stars (0.8-8 M_⊙). Oxygen abundance (log[O/H]) obtained from nebular spectral emission lines can be assumed roughly invariant for AGB evolution in the Galaxy [1], therefore indicative of the in-situ oxygen abundance at the time of formation of the stellar progenitor, modulo subsequent dynamical evolution. By comparing radial metallicity gradients of different age groups of progenitors, one can study chemical evolutionary models of the Galaxy.

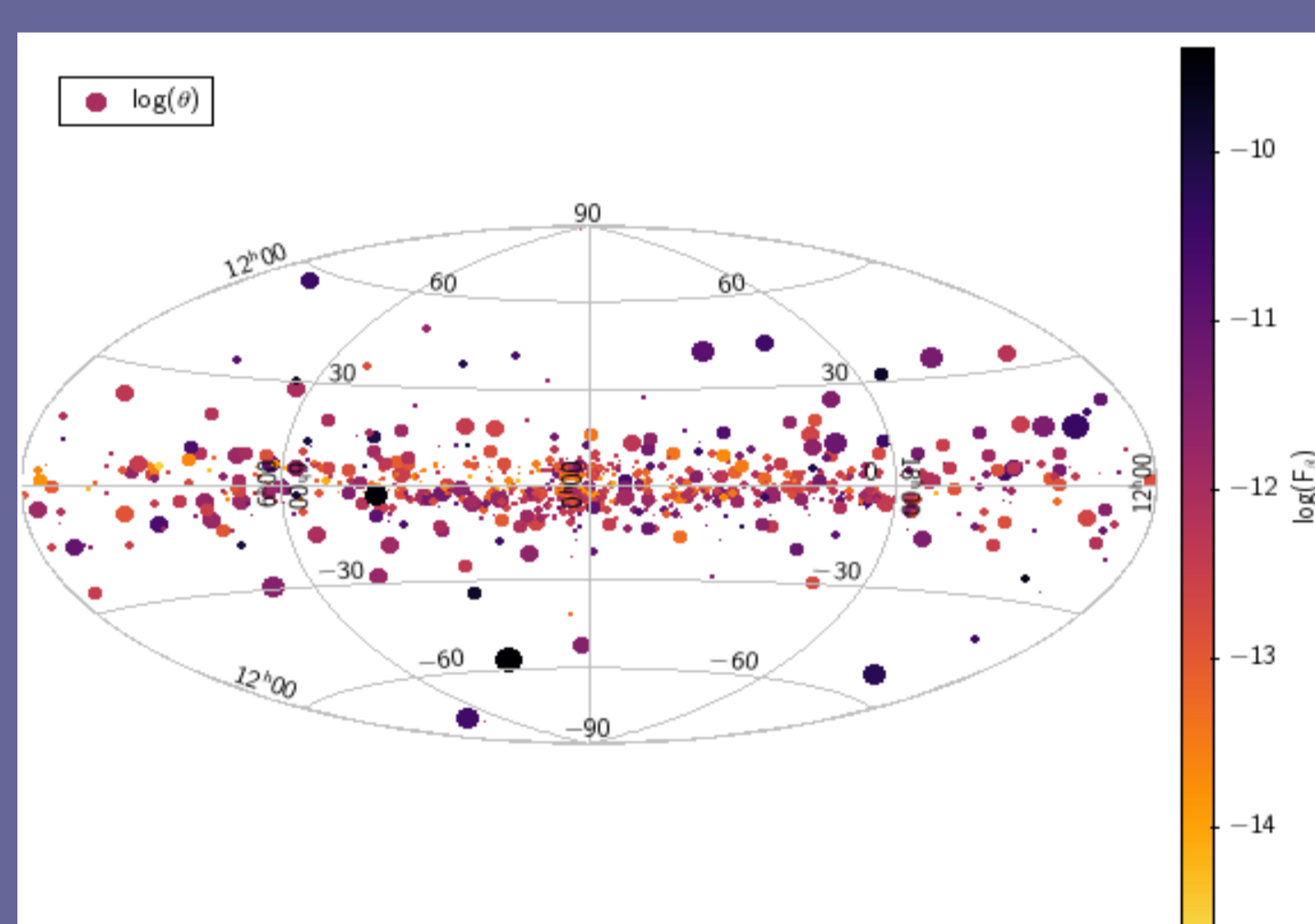
PN DATASET and DR3 CALIBRATORS



- (A) 2556 original target list of true planetary nebulae (PNe) extracted from the HASH database [2]
- (B) 942 central stars (CSPNs) astrometrically cross-matched with Gaia DR3, also found in Gonzalez-Santamaria et al. [3] and Chornay & Walton [33] catalogs, whose unique matches are also based on Gaia BP-RP colours
- (C) 843 PNe from the original target list with angular radius and surface brightness data
- (D) 306 PNe from the original target list with Oxygen and Nitrogen chemical abundances data (62 of them also have Carbon abundances)
- (B) ∩ (C) → 472 CSPNs potential calibrators for the new distance scale
- (C) ∩ (D) → 283 PNe sample used to trace the radial metallicity gradient



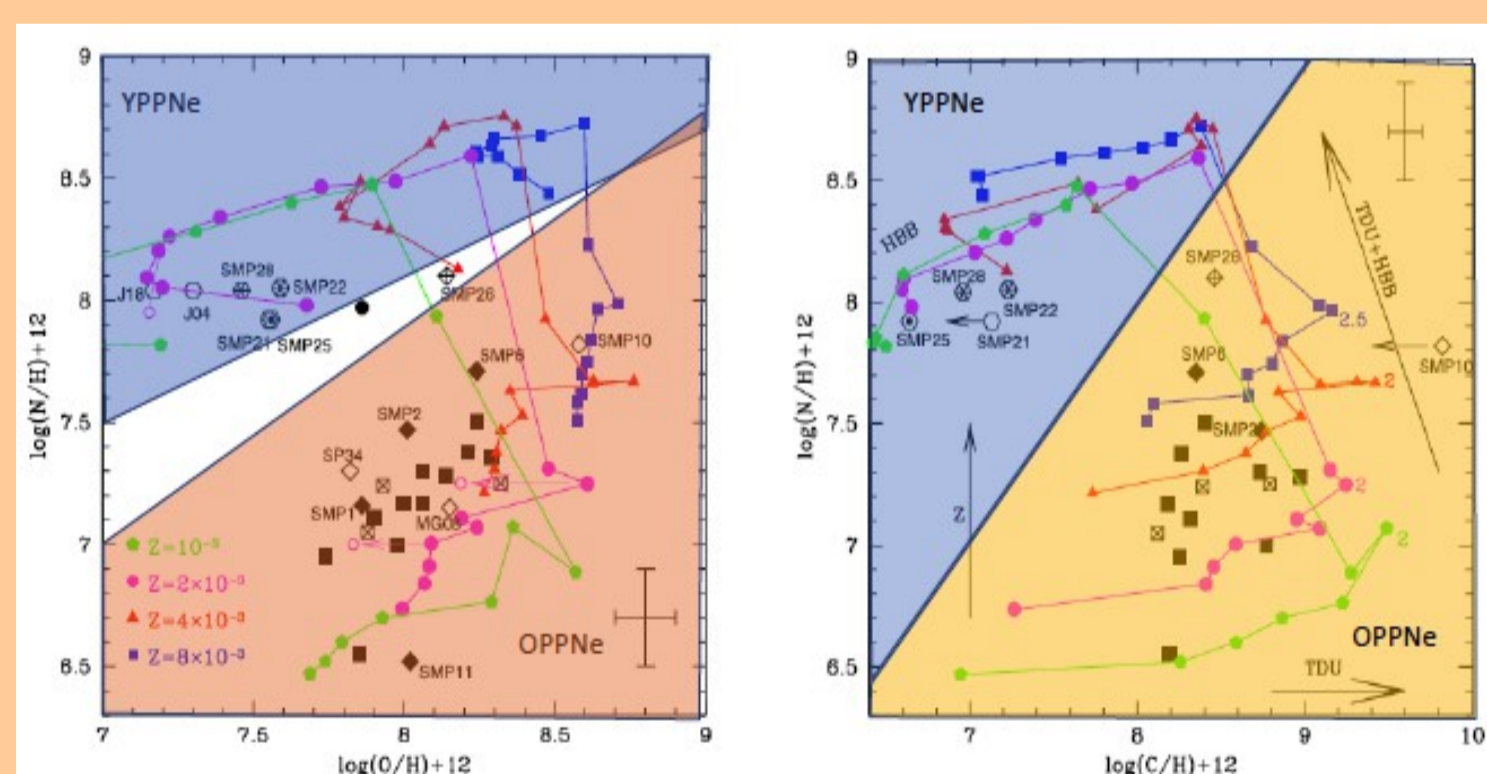
G magnitude distribution of the full PNe sample matched with Gaia DR3, and of the subset of potential distance calibrators, before any threshold is applied on the relative DR3 parallax error.



Galactic coordinates (Aitoff projection) of the 843 (C) PNe set with flux and angular radius data. The points' size is proportional to the logarithm of the nebula's angular radius (arcseconds) and the color range reproduces the logarithmic H β flux (erg cm⁻² sec⁻¹)

DATING PNe PROGENITORS

The two graphs adapted from Ventura et al. [11] show the evolutionary yields of CNO elements for different asymptotic giant branch (AGB) stellar models. Lines of different colours connect models of fixed metallicity (Z) and different masses in the range 0.9 M_⊙ < M < 8 M_⊙, with masses increasing counterclockwise for each track.



From the inspection of these graphs, we observe that PNe with young and old CSPN progenitors occupy different loci on the N/H vs. C/H and O/H vs. N/H planes, as highlighted by the shaded areas. Among the PNe for which we have chemical abundances, we identify 191 and 56 PNe with progenitors of age > 7.5 Gyr (OPPNe) and < 1 Gyr (YPPNe), respectively

NEW DISTANCE SCALE PARAMETERS

- From the 472 CSPNs, we apply a selection threshold based on the DR3 relative parallax error, namely 5%, 10% and 20%, ending up with 26, 74, 137 calibrators respectively

- The distance scale parameters are inferred from the semi-empirical *log-linear* relationship between the physical radius and the surface brightness of the nebula [5,6]:

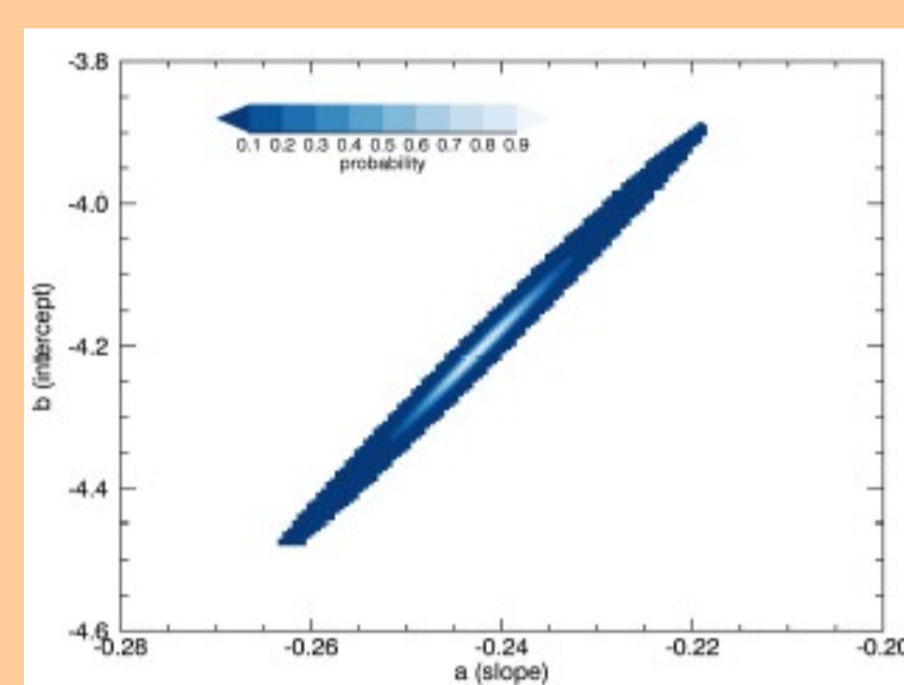
$$\log(R) = a \log(S_{H\beta}) + b$$

where (a, b) are the slope and intercept of the straight line, while R and SHBeta are functionally related to the observed angular radius (θ), flux (I) and parallax (ω).

- We apply the bayesian inference model detailed in [7] to infer the posterior probability density function p(a,b| ω, θ, I), and derive their confidence intervals and correlation.

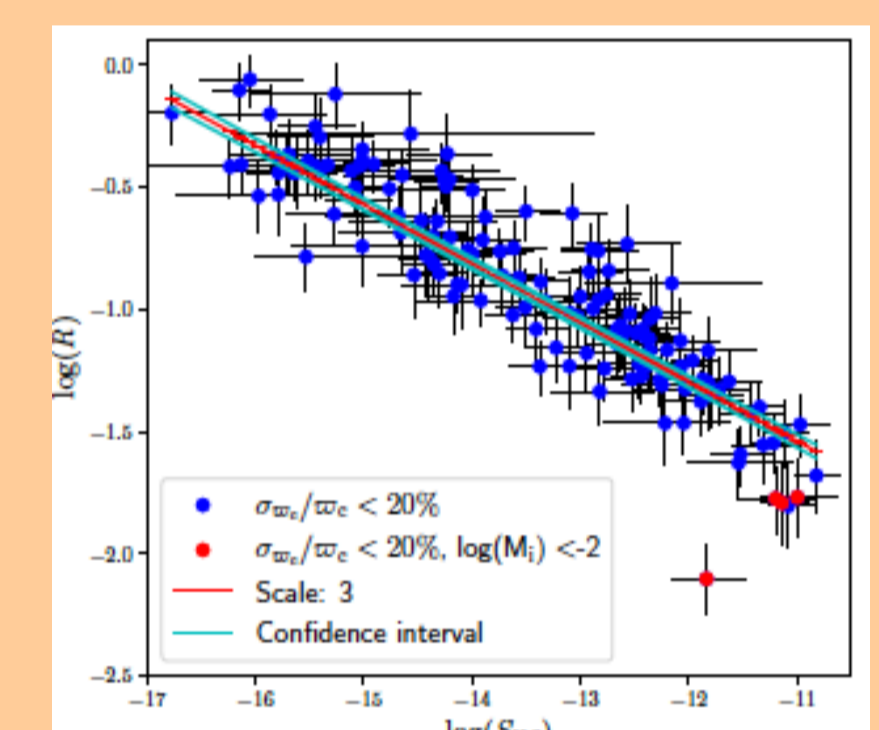
- We adopt the scale parameters' values inferred from the 20% parallax relative error calibrator sample, obtaining

$$a = -0.242 \pm 0.004, b = -4.20 \pm 0.057, \rho_{ab} = 0.99$$



2D posterior distribution of scale parameters

log(R)-log(S_{Hβ}) plot for calibrators with relative parallax error < 20%



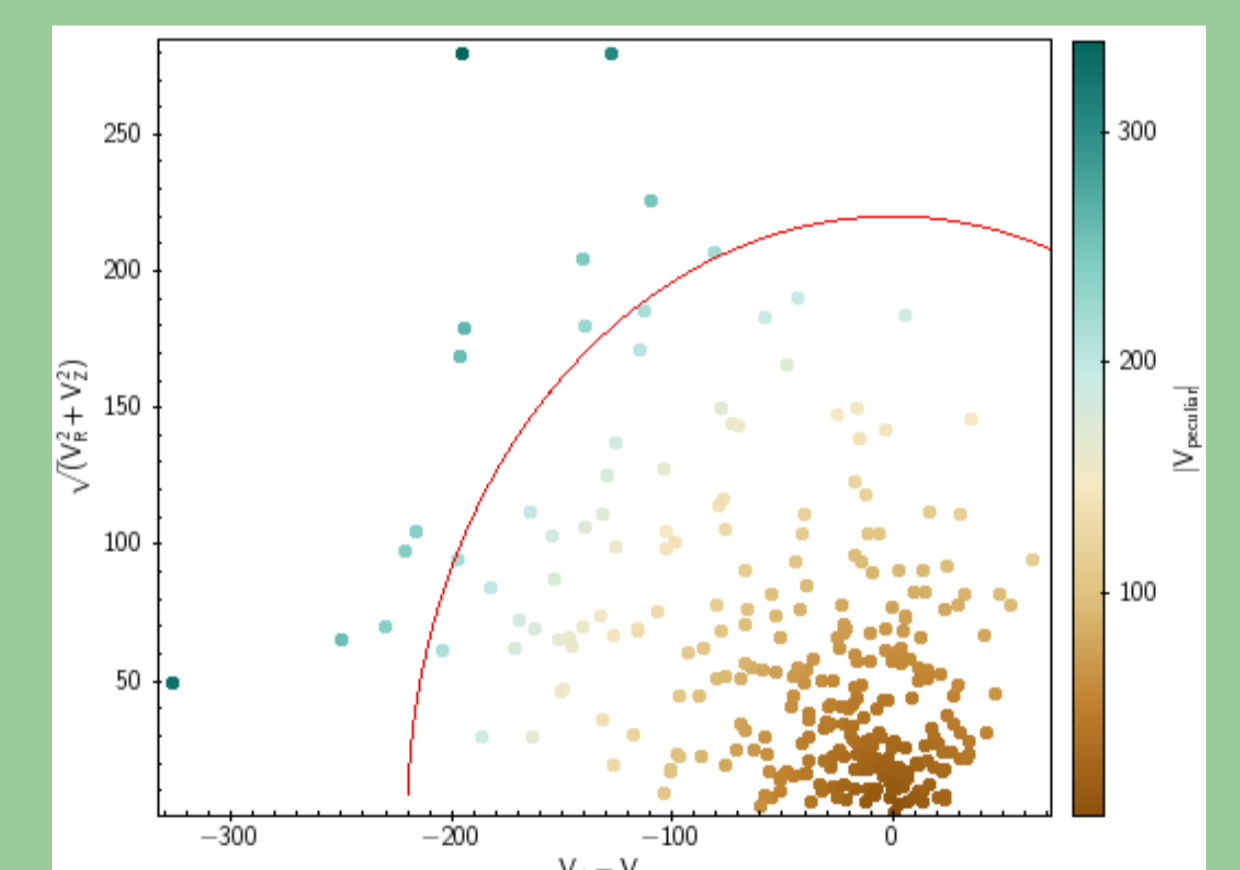
KINEMATICS OF PNe CENTRAL STARS

We compute the space motions for 297 CSPNe by combining radial velocities taken from literature data [8] with Gaia DR3 proper motions.

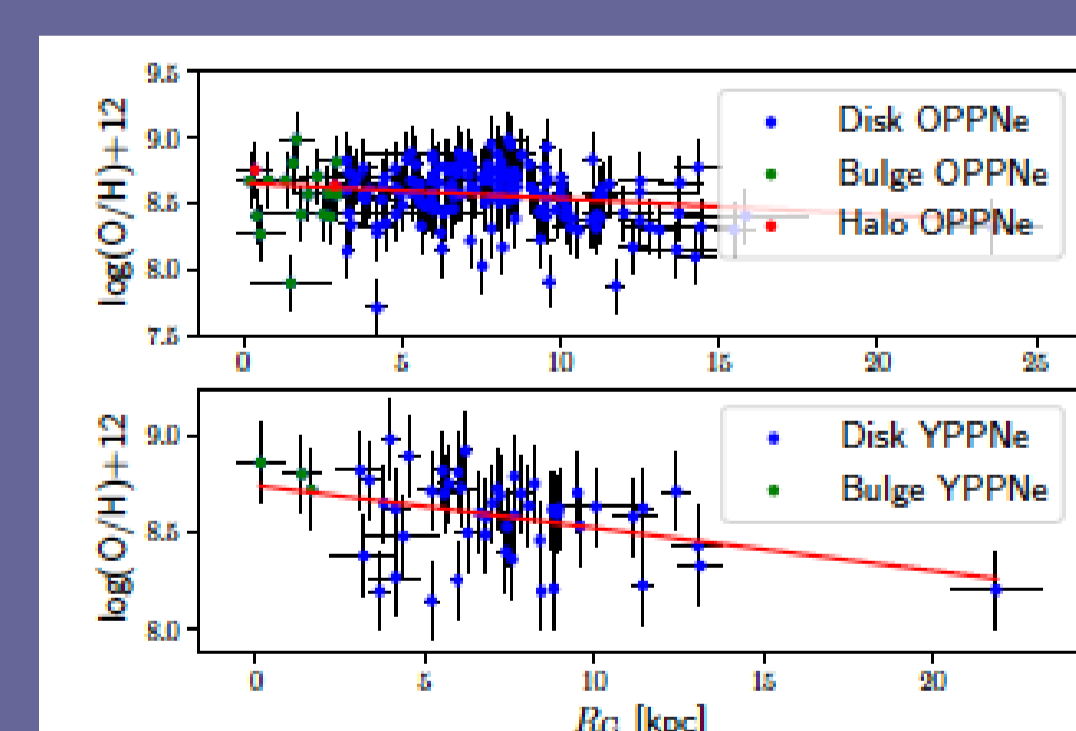
By using an empirical model for the Galactic rotation curve adapted from [9,10], with fundamental parameters

R₀ = 8.122 kpc, V_{LSR} = 229 km/s, we derive the galactocentric radial, azimuthal, and vertical components of the peculiar velocities V_R, V_ϕ, V_z

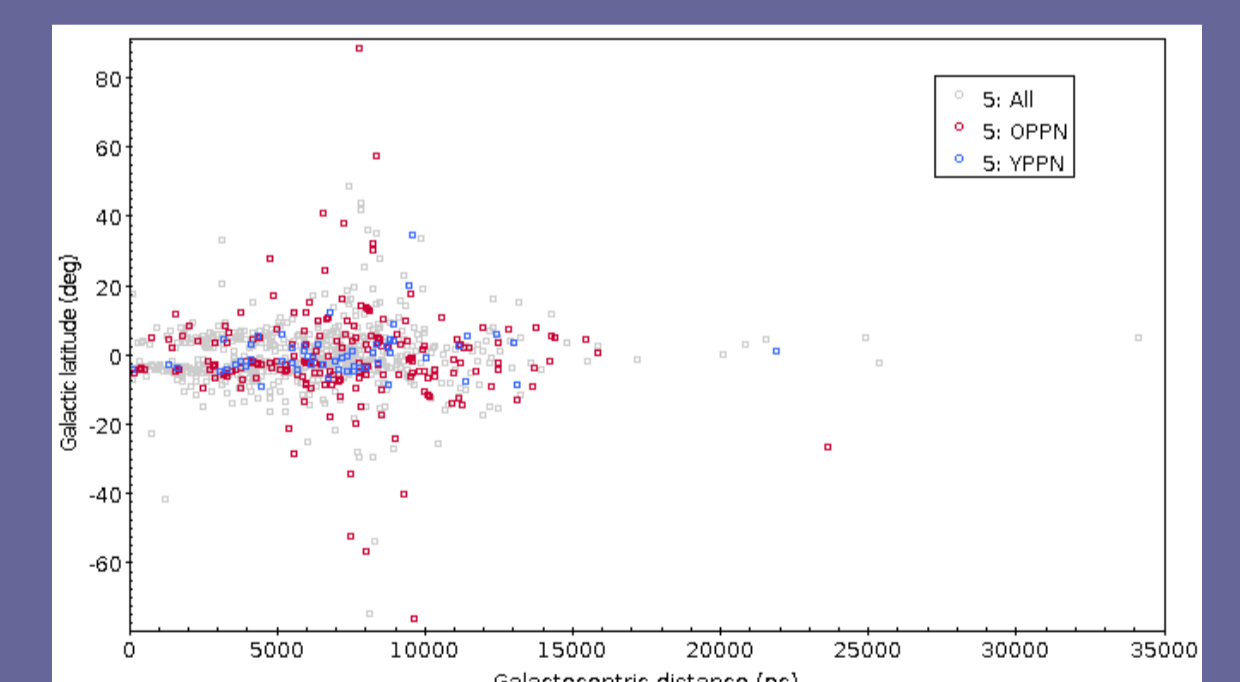
We use these velocities to build the so-called Toomre diagram to identify the region of high probability of finding Halo stars (outside the red circle in the picture), which we take out from our subsequent analysis. The red circle correspond to peculiar velocities of 220 km/s



RADIAL METALLICITY GRADIENTS



Radial oxygen gradients for the OPPNe (top) and YPPNe (bottom) populations. Chemical abundances are averaged when one more than one datum is available from the literature, and the error bars represent the dispersion.



Galactocentric distances of the sample of 297 PNe for which both physical parameters and chemical abundances are available, and of the 56 YPPNe and 191 OPPNe identified from the log[O/H], log[N/H], log[C/H] relative values (see details on the left panel)

RESULTS We fit a linear gradient $\Delta \log[O/H] / \Delta R_0$ along the Galactic disk estimating a slope of -0.0121 ± 0.0046 and -0.022 ± 0.0076 (dex kpc⁻¹) for the old (> 7.5 Gyr) and young (< 1 Gyr) population respectively. These negative, shallow gradients disclose a mild steepening of the slope since Galaxy formation, confirming other studies based on gas-phase metallicity data [12,13,14].

REFERENCES:

- [1] Stanghellini L. and Haywood, M. 2018, ApJ 862:45.
- [2] Parker Q.A. et al. 2016, Journal of Physics Conference Series, 728.
- [3] Gonzalez-Santamaria J. et al. 2021, A&A 656, 51.
- [4] Chornay N. and Walton N.A. 2021, A&A 656, 110.
- [5] Shklovsky I.S. 1956, AZh, 33, 315.
- [6] Bensby T. and Lundstrom I. 2001., A&A 374, 599.
- [7] Stanghellini L., Bucciarelli B., et al. 2020, ApJ, 889, 21.
- [8] Durand S. et al. 1998, A&AS 132, 13.
- [9] Eilers A.-C. Et al 2019, ApJ 871, 120.
- [10] Bhattacharjee P. et al. 2014, ApJ 785, 63.
- [11] Ventura, P. et al. 2016, MNRAS 460, 3940.
- [12] Pena M. and Flores-Duran S.N. 2019, Rev. Mexicana Astron. Astrofis. 55,255, 2019
- [13] Bhattacharya S. et al. 2022, MNRAS 517: 2343.
- [14] Lian J. et al. 2023, Nature Astronomy 2023 [arXiv:2306.14109]